MATERIALS CHEMISTRY COMMUNICATION

Enhanced fluorescence of coumarin laser dye in the restricted geometry of a porous nanocomposite

P. Wlodarczyk, S. Komarneni,* R. Roy and W. B. White

Intercollege Materials Research Laboratory, The Pennsylvania State University, University Park, PA 16802, USA

We report here the dramatic increase in fluorescence intensity of 7-diethylamino-4-methylcoumarin (coumarin 1) laser dye in the restricted geometry of a pillared clay nanocomposite. The fluorescence intensity of the alumina-pillared fluorphlogopite–coumarin complex is about 6 times greater than that of the fluorphlogopite–coumarin complex. The prevention of dye aggregation and the change of the crystal field surrounding the coumarin dye molecules in the compartments between pillars apparently lead to this fluorescence enhancement. The positive results obtained here may lead to the potential application of dye-intercalated nanocomposite clays in linear and non-linear optics.

Lasers depend on an amplifying medium for their operation. In dye lasers this medium is a solution of an organic dye. The original dye laser employed a phthalocyanine solution,[1] but this solution was soon replaced by rhodamine 6G[2] which is still one of the most widely used amplifying dyes today. After the development of the dye laser, thousands of dyes were investigated for this purpose. With such intensive investigation of available dye sources, it was determined that only four additional and previously commercially available dyes, pyronin B, rhodamine S, 9-aminoacridine hydrochloride and benzyl β-methylumbelliferone, were useful in the dye laser.[3] A vast amount of research has been carried out to date on the structure and fluorescence of laser dyes and these properties are well established.

It is well known that fluorescence efficiency is high in dye molecules with rigid, planar structures[4] and that aggregation of dye molecules has a major role in fluorescence quenching. Dyes that form dimers and larger aggregates will often have distinctly different absorption bands. Some may have weak or no fluorescence at all. In general, dyes aggregate to a greater extent in water than in organic solvents. Aqueous concentrated dye solutions show less aggregation in the presence of alcohol or glycerol.[5] Where an aqueous solution is desired for xanthine dyes, surfactants such as hexadecyltrimethylammonium bromide, Triton X, sodium lauryl sulfate and potassium oleate have been studied with varying degrees of success.[6] One of the effective ways to prevent dye aggregation is to isolate the molecules in a matrix. In the last decade, several studies of the effects of restrictive geometries on optical dyes have been performed. The majority of these studies used sol–gel-processed alumina films and silicate gels as the host matrices for the dye.[7–10] In these studies, sols were doped with various organic dyes and gelled to trap the dye within the microporous gel structure. Other studies were performed on swelling clays with organic dyes intercalated within the 2:1 structure of the phyllosilicate.[11] The concentration of dye solutions and cation-exchange capacity of the clay were the controlling factors for the amount of intercalated dye. The novel crystal-field environment of the gels and clays in these studies was reported to increase the melting temperature and to affect the fluorescence intensity and photostability of the intercalated dyes. The conceptual innovation in the present work was to create a nanocomposite of dye molecules in the restricted compartments in a porous, pillared clay.

Natural phyllosilicates, including montmorillonite from three different sources, a saponite, a hectorite, a synthetic lithium fluorhectorite (Corning) and a synthetic sodium fluorphlogopite (Kunimine), were intercalated with the Al_{13} polymer $\{[Al_{13}O_4(OH)_{24}(H_2O)_{12}]^{7+}\}$ precursor and calcined to yield alumina-pillared clay nanocomposites. The pillaring of clays is now an established process.[12–14] Successful pillar formation was tested by X-ray analysis. Basal spacings of the pillared phyllosilicates ranged from 16.9 to 18.1 Å after pillaring and heating at 450 °C for 5 h (Table 1). These basal spacings are typical of clays pillared with alumina.

Both the original phyllosilicates and their corresponding pillared nanocomposites were intercalated with the laser dyes, 7-diethylamino-4-methylcoumarin (coumarin 1; hereafter coumarin), pyronin Y, rhodamine B and rhodamine 6G in solutions of ethanol. Equivalent processing techniques were employed for all samples to introduce the laser dyes into the interlayer. The only significant differences in intercalation were introduced in the dye solution concentrations to accommodate the difference in cation-exchange capacities (CECs) between pillared samples and the corresponding non-pillared component phyllosilicates. Table 1 lists the CEC values determined by a standard procedure[15] for each phyllosilicate and subsequent nanocomposite used. It is apparent that between 60 and 87% of the CEC was satisfied by pillar species in the

Table 1 Cation-exchange capacity (CEC) of pillared and non-pillared phyllosilicates

	CEC of sample		
phyllosilicate	non-pillared/ mequiv (100 g)$^{-1}$	pillared/ mequiv (100 g)$^{-1}$	basal spacing of pillared clay/Å
1 Kunipia montmorillonite (Japan)	126	22	17.6
2 saponite (CA)	101	40	16.9
3 lithium fluorhectorite (synthetic)	200	59	17.3
4 sodium fluorphlogopite (synthetic)	79	25	18.1
5 Texas montmorillonite (TX)	128	17	17.3
6 hectorite (CA)	92	37	16.9
7 Arizona montmorillonite (AZ)	115	27	17.7

interlayer The CEC remaining in the phyllosilicate layers aids in the intercalation of the dye molecules which are cationic in solution The uptake mechanism of neutral dyes such as coumarin (although charge can develop with pH changes) is not understood but could be due to the hydrophobic nature of the interlayer surface

The dye intercalation procedure used was as follows Ethanol–water solutions of each laser dye (0 16 mol l^{-1}) were prepared to satisfy 200% of the CEC in the highest-charged phyllosilicate, fluorhectorite The other phyllosilicates were treated with the same concentration of laser dye, assuming any excess dye would be removed by washing prior to optical and thermal analysis Similarly, a 0 048 mol l^{-1} solution of dye and EtOH–H_2O (95 5, v/v) was prepared to satisfy 200% of the CEC remaining in the highest-charged pillared phyllosilicate, fluorhectorite, and in excess for the other pillared samples Prior to solution preparation, it was determined that the solubility of these solutions was better in ethanol than in water Each dye solution was stirred in a sealed container for several hours to ensure good dissolution

Approximately 0 2 g of each original and pillared phyllosilicate were weighed and placed in 35 ml plastic bottles for each of the four dye solutions The dye solutions (0 16 mol l^{-1}, 25 ml) were pipetted into each original phyllosilicate Similarly, 25 ml of 0 048 mol l^{-1} dye solutions were pipetted into each pillared phyllosilicate All of the samples were shaken vigorously for 1 min and placed in a test-tube rack rotator for more than 1 day in a closed cabinet to decrease any light degradation of the dye molecules in solution The 28 samples were then placed in a 65 °C water bath for 1 week, and again protected from light exposure Upon removal from the water bath, each sample was vacuum-filtered and rinsed with ethanol several times until the filter run-off appeared clear, indicating the removal of most of the excess dye that was not held in the interlayer The pillared phyllosilicate–dye and phyllosilicate–dye complexes were left upon the PTFE membrane filter and placed in a closed cabinet to dry in the air at room temperature for more than 24 h The dye-intercalated samples were then placed in small glass vials and sealed for later testing

The optical properties of bulk dye solutions and dye–phyllosilicate complexes were analysed using a Hitachi fluorescence spectrophotometer, model number F-4010 Dye solutions used for the intercalation procedure were analysed first Dilute solutions, *ca* 10^{-4} mol l^{-1}, of dye and ethanol show the least amount of quenching due to dimer and trimer formation [5] With this in mind, the 0 048 mol l^{-1} dye solutions were placed in quartz vials and analysed several times with continuous dropwise dilution and agitation All of the dye solutions exhibited a slight blue shift and peak intensity increase with dilution When this behaviour ceased, the spectra obtained were stored The excitation wavelengths, λ_{exc}, of incident light used for coumarin, pyronin Y, rhodamine B and rhodamine 6G were 370, 360, 550 and 530 nm, respectively The reported λ_{exc} values were adjusted to produce the most intense peak by running the dye solutions at the given wavelength and investigating 5 nm shifts about the value, totalling a 50 nm span to each side The ethanol solution used to produce the dye solutions was tested at each of the four excitation wavelengths, to ensure that any Raman peaks due to the solvent were not misinterpreted as dye fluorescence A Raman peak was only evident in the pyronin Y solution at 431 nm, this peak was much less intense than the fluorescence peak at 588 nm and was disregarded in further testing of pyronin Y complexes

Dye complexes of phyllosilicate and pillared phyllosilicate were analysed at the excitation wavelengths attained in the dye solution study Each sample was placed in a solid sample holder behind a quartz window and fluorescence spectra collected, again in the range 220–700 nm Data were also collected for the phyllosilicates and nanocomposites that were not dye-intercalated at the four excitations used in the dye studies Owing to the temperature dependence of fluorescence, room temperature was monitored during analysis Temperatures were 19±1 °C for the duration of the data collection and significant fluctuations in fluorescence were not detected

Differential thermal analysis (DTA) was used to investigate the changes in melting and decomposition temperature of intercalated dyes A platinum sample cup was filled with each of the dye-intercalated samples and the bulk dye in powder form and run from 50 to 650 °C at a rate of 10 °C min^{-1} *vs* an aluminium oxide standard A Perkin-Elmer DTA model 1700 in tandem with a system 7/4 thermal analysis controller and a data station equipped with Perkin-Elmer TADS software was used to collect all data

Detailed fluorescence results of the various dye–clay and dye–pillared clay complexes, apart from the coumarin complexes, do not justify detailed presentation The results show that pyronin Y exhibited no fluorescence in complexes of pillared and non-pillared phyllosilicates while rhodamine B and rhodamine 6G intercalates in either unpillared or pillared clays showed no fluorescence improvement

All the unpillared clay–coumarin dye complexes exhibited relative intensity increases over the unpillared clay–dye composites when fluorescence tested at λ_{exc}=370 nm Maximum fluorescence intensity occurred between 443 and 498 nm Each set of spectra was obtained at an excitation and emission bandpass to maximize the fluorescence emission without saturating the detector Therefore intensities within each data set can be compared Table 2 summarizes the fluorescence data obtained for coumarin The fluorescence peak width at half maximum intensity (FWHM) was measured from each curve (within ±2 nm)

Because the actual molecular concentration of dye molecules in the original and pillared clays is not known, quantum efficiencies cannot be calculated Because of the differences in scattering characteristics and the unknown concentrations, it is likewise not possible to compare the fluorescence intensities of dye–clay complexes with the dye solutions However, with care in packing the clays into the sample cell and making the measurements with the same instrument settings, the

Table 2 Fluorescence data for clay–coumarin complexes

phyllosilicate of dye complex	λ^a/nm	intensity[b]	enhancement[c]	FWHM/nm
1 original, pillared	469, 451	66, 135	—, 2 05	62, 51
2 original, pillared	467, 455	343, 644	—, 1 88	55, 51
3 original, pillared	469, 452	370, 2590	—, 7 0	52, 78
4 original, pillared	465, 443	1303, 7829	—, 6 01	49, 80
5 original, pillared	474, 452	265, 1417	—, 5 35	52, 56
6 original, pillared	498, 445	528, 2916	—, 5 52	51, 56
7 original, pillared	458, 453	189, 350	—, 1 85	51, 60

[a]Wavelength at maximum intensity [b]Relative intensities for all specimens measured in the same way with the same instrument settings [c](Fluorescence intensity of pillared clay)/(fluorescence intensity of original clay–coumarin complex)

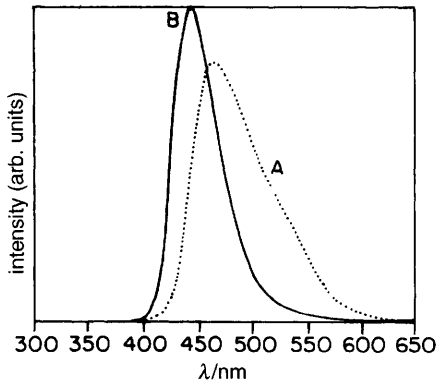

Fig. 1 Fluorescence emission spectra for (A) sodium fluorphlogopite–coumarin complex (intensity magnified 5×) and (B) pillared sodium fluorphlogopite–Coumarin complex. Excitation wavelength = 370 nm.

Table 3 Bulk dye and dye–complex melting temperatures

sample	complete melting[a]/°C	melting temp. increase[a,b]/°C
bulk coumarin dye	85	
dye–**1** complex	92; 157	7; 72
dye–**2** complex	176; 177	91; 92
dye–**3** complex	198; 154	113; 69
dye–**4** complex	93; 100	8; 15
dye–**5** complex	120; 163	35; 78
dye–**6** complex	112; 146	27; 61
dye–7 complex	183; 168	98; 83
bulk pyronin Y dye	280	
dye–**1** complex	320; 316	40; 36
bulk rhodamine B dye	210	
dye–**1** complex	253; 270	43; 60
bulk rhodamine 6G dye	264	
dye–**1** complex	275; 270	11; 6

[a]Original; pillared. [b]Increase over bulk dye melting temperature.

comparison between the pillared clays and the original clays should be reasonably accurate.

Fluorescence intensity was greatly enhanced in all pillared phyllosilicate–coumarin complexes (Table 2). The pillared fluorhectorite–coumarin complex exhibited an intensity *ca.* 7 times that of the non-pillared fluorhectorite–coumarin complex, and over 6 times that of the non-pillared fluorphlogopite–coumarin complex was attained in the pillared sodium fluorphlogopite–coumarin complex (Fig. 1; Table 2). This dramatic enhancement in fluorescence may be attributed to the isolation of coumarin molecules in the compartments between pillars with little or no interaction between the molecules. The pillaring of layers also leads to a lower CEC and therefore, the number of molecules that enter the interlayers is also limited. The smaller number of molecules coupled with their isolation in the compartments appears to cause this dramatic increase in fluorescence. The red shift evident in the non-pillared phyllosilicate–coumarin complexes (Table 2; Fig. 1) is an indication that the adsorbed dye is located in the interlayer space of the phyllosilicate. Similar red-shift changes were reported by Endo *et al.*[11] for pyronin Y and rhodamine 590 intercalated in montmorillonite.

Thermal analysis showed that the intercalated dye molecules in pillared clay nanocomposites have substantially higher thermal stability than those intercalated in non-pillared clays (Table 3). In general, dye molecules intercalated in clays have a higher thermal stability than those in dye alone.

Although the positive results presented in this research are limited to coumarin complexes, the data provided suggest several potential applications of dye-intercalated nanocomposites as laser light guides and filters in linear and non-linear optics.

This research was supported by the Division of Materials Science, Office of Basic Energy Sciences, US Department of Energy under grant no. DE-FG02-85ER45204.

References

1 P. P. Sorkin and J. R. Lankard, *IBM J. Res. Develop.*, 1996, **10**, 162.
2 P. P. Sorkin, J. R. Lankard, E. C. Hammond and V. L. Moruzzi, *IBM J. Res. Develop.*, 1967, **11**, 130.
3 D. W. Gregg and S. J. Thomas, *IEEE J. Quant. Electr.*, 1969, **5**, 302.
4 Th. Foster, *Fluoreszenz Organischer Verbindungen*, Vandenhoeck and Ruprecht, Göttingen, 1951, pp. 94–124.
5 O. Valdes-Aguilera and D. C. Neckers, *Acc. Chem. Res.*, 1989, **22**, 171.
6 V. K. Kelkar, B. S. Valaulikar, J. T. Kunjappu and C. Manohar, *Photochem. Photobiol.*, 1990, **52**, 717.
7 D. Avnir, D. Levy and R. Reisfeld, *J. Phys. Chem.*, 1984, **88**, 5956.
8 J. Warnock, D. D. Awschalom and M. W. Shafer, *Phys. Rev.*, 1986, **34**, 475.
9 J. C. Pouxviel, S. Parvaneh, E. T. Knobbe and B. Dunn, *Solid State Ionics*, 1989, **32/33**, 646.
10 H. Tanaka, J. Takahashi and J. Tsuchiya, *J. Non-Cryst. Solids*, 1989, **109**, 164.
11 T. Endo, N. Nakada, T. Sato and M. Shimada, *J. Phys. Chem. Solids*, 1988, **49**, 1423.
12 S. Yamanaka, *Ceram. Bull.*, 1991, **70**, 1056.
13 P. Malla, S. Yamanaka and S. Komarneni, *Solid State Ionics*, 1989, **32/33**, 354.
14 P. B. Malla and S. Komarneni, *Clays Clay Miner.*, 1990, **38**, 363.
15 M. L. Jackson, *Soil Chemical Analysis—Advanced Course*, 2nd edn., The University of Wisconsin, Madison, WI, 1979, p. 895.

Communication 6/05603B; *Received* 12*th August*, 1996